

Risk-based truck-drone delivery optimization

Wenxuan Wang, Mai Zhang, Ethan Beech, Arnab Majumdar, Washington Ochieng, Jose Escribano

*Extended abstract submitted for presentation at the 12th Triennial Symposium on Transportation Analysis conference (TRISTAN XII)
June 22-27, 2025, Okinawa, Japan*

February 15, 2025

Keywords: last-mile delivery, truck-drone delivery, drone risk assessment, vehicle routing, drone pathfinding

1 INTRODUCTION

The global last-mile delivery market was valued at \$40 billion in 2021. The rise of e-commerce has further increased its importance in recent years, with last-mile delivery costs up to 53% of total logistics costs. For this reason, logistics enterprises are seeking to incorporate new autonomous technologies that improve delivery times and reduce driver salary expenses. Among these technologies, drones are increasingly seen as credible alternatives to conventional last-mile distribution, with companies like Amazon, DHL, and Google having presented prototypes in recent years. In fact, (Raghunatha *et al.*, 2023) concludes that electric drones are faster and may be more economically cost-effective than trucks for last-mile delivery services.

However, incorporating drones into last-mile distribution is no trivial task. The modeling of hybrid truck-drone delivery services has given rise to the flying sidekick problem, a variant of the Traveling Salesman Problem (TSP), which facilitates the coordinated deployment of drones and trucks. Approaches to this problem, including (Murray & Raj, 2020), (Jeong *et al.*, 2019), and (Zhe & HERVE, 2022), typically employ common cost-minimization objectives found in classical logistics research. As a result, they overlook the significant safety risks drones pose when operating over urban landscapes and fail to consider that routing and pathfinding can greatly influence risk, potentially jeopardizing operational viability. While studies such as (Ren & Cheng, 2020), (Jeong *et al.*, 2021), and (Pang *et al.*, 2020) have developed initial methods for estimating drone operational risk, they are limited in their ability to model risk factors and levels comprehensively. For example, (Pang *et al.*, 2020), as the most advanced study among them, features a risk-aware path planning model. However, it categorizes risk into five predefined levels based solely on incident probability, rather than systematically assessing both the probability and severity of incidents using precise values. This creates a significant limitation within the risk model. To address these gaps, we introduce our systematic risk model for drone operations and apply it to optimize the hybrid truck-drone network for urban last-mile deliveries.

2 MODEL FORMULATION

This section outlines the drone operational ground risk model, the risk-aware truck-drone routing model, and the risk-aware drone pathfinding model. A sequential optimization approach is employed, with the drone path being optimized separately in the third model.

The aim of establishing a drone ground risk model is to produce a risk grading R_g for each grid cell g within a given area, quantified by the predicted number of lethal injuries to people in grid

g posed by drones flying over it. The value of R_g is obtained by multiplying the likelihood and severity of potential injuries, as defined in Equation 1. For each grid g , we estimate the likelihood $L(g)$ of lethal injuries to people in it based on a normal distribution for the crash area of a failing drone, the grid's population density ρ_g , and the drone's failure rate p_g . Severity calculation begins by determining the drone's impact energy E_{imp} , which depends on the landing position relative to the failure's starting location. Each grid g is then categorized as either road (x_r , for vehicles), pavement (x_p , for pedestrians), or building (x_b) based on its location. x_r , x_p , and x_b are binary variables; when one of them equals 1, the others must equal 0. Any direct impact on the pavement x_p is assumed to cause fatalities to the pedestrian(s) in grid g , while vehicles on the road x_r are considered unaffected by any drone with an impact energy E_{imp} below the regulatory energy absorption standard E_{absp} . For people inside the building x_b , severity also depends on the drone's loading factor M , characteristic dimensions D , and the building's structural energy resistance capability E_{res} . When a drone failure impacts the building roof, the drone's loading factor M is further influenced by its loading modes, including point loading, distributed loading, or helipad loading. If the crash occurs at the glass wall, the probability of glass fracture is also considered. The final risk level R_g is then used in the routing and pathfinding process, combined with the operational time to optimize the route network and path.

$$R_g = L(g)S(g) = p_g \rho_g x_p + \mathbb{I}(E_{imp} > E_{absp})x_r + MD^2\mathbb{I}(E_{imp} > E_{res})x_b \quad (1)$$

The routing model is designed to identify the optimal node visiting sequence for trucks and drones while avoiding drone deliveries to the riskiest grids. It is formulated as a TSP with the objective of minimizing both operational time and risk (see Equation 2). These two factors are then scaled into a single aggregate objective function to balance them, which is a commonly used approach in hybrid-objective optimization. Finally, w_1 , w_2 , and w_3 are set to 0.30, 0.40, 0.35, respectively, to scale and adjust their relative importance. The first and second terms together represent the total operational time for the truck and drone, where x_{ij} indicates whether nodes i and j are connected by truck, y_{ijk}^D denotes whether a drone launched from node i travels to node j before returning to the truck or the ending depot at k , and θ_{ij}^T and θ_{ij}^D represent the operational time between nodes i and j for trucks and drones, respectively. Since the full trajectory has not yet been determined, the shortest road and straight-line aerial paths between the nodes are used to calculate the truck and drone operational time, respectively.

The third and fourth terms represent the drone operational risk, along the path and during customer service, respectively. Here, z_i^D is a binary variable that equals 0 or 1, indicating whether customer node i is accessed by a drone. As defined by our ground risk model, R_i^D denotes the risk of a drone operating above the node i . Since our approach measures risk in grids, R_{ij}^D , which represents the total risk of a drone operation from node i to node j , is calculated by summing the risk R_i^D of the drone operating at each trajectory vertex relative to the ground grids. The likelihood of a drone failure for each grid and its corresponding severity are both derived from the ground risk model.

$$\min w_1 \times_{i \in 2N, j \in 2N, i \neq j} x_{ij}^T \theta_{ij}^T + w_2 \times_{i \in 2N, j \in 2C, k \in 2N_+} y_{ijk}^D (\theta_{ij}^D + \theta_{jk}^D) + w_3 \times_{i \in 2N, j \in 2C, k \in 2N_+} y_{ijk}^D (R_{ij}^D + R_{jk}^D) + \times_{i \in 2C} z_i^D R_i^D \quad (2)$$

During the delivery process, the drone must depart from and return to the truck at customer nodes to ensure the drone landing coincides with the truck parking. Equations 3 and 4 define the specific constraints applied to consider two conditions: a drone can only land on buildings with a balcony or courtyard; packages that require a signature must be delivered by a human-driven truck. The remaining constraints, not shown here, are obtained from Murray & Raj (2020).

$$\times_{j \in 2C, i \notin j} \times_{k \in 2N_+} y_{ijk} = 1 \quad \forall i \in 2N_0 \quad (3)$$

$$\prod_{i \in N_0, i \neq k} \prod_{j \in C} y_{ijk} \quad 1 \quad \delta_k \geq N_+ \quad (4)$$

After determining the route network, the drone pathfinding model optimizes drone paths along these routes to minimize both path length and operational risk, utilizing the risk matrix and Dijkstra algorithm, as shown in Equation 5. In this model, $\|x_i(s_{k+1}) - x_i(s_k)\|$ represents the Euclidean distance between two consecutive states s_k and s_{k+1} along a path, while $R(x_i(s_k))$ denotes the risk associated with the position of the drone i at the state s_k .

$$\min \sum_{i \in N, k \in K} \|x_i(s_{k+1}) - x_i(s_k)\| + \sum_{i \in N, k \in K} R(x_i(s_k)) \quad (5)$$

3 RESULTS

We applied the proposed approach to a 30-customer instance in the western London area, covering 0.382 km² in Hounslow and Richmond upon Thames. The depot location was set based on an existing operational DHL warehouse depot at N51 27.45^o, E0 23.36^o.

The study area was discretized into a 44 × 46 grid map for drone operational risk modeling. This simulation assumed an average operating speed of 18 km/h for trucks in the last-mile stage. For all drone deliveries, the DJI FlyCart 30 was used, operating at 90% of its maximum speed, equivalent to 18 m/s.

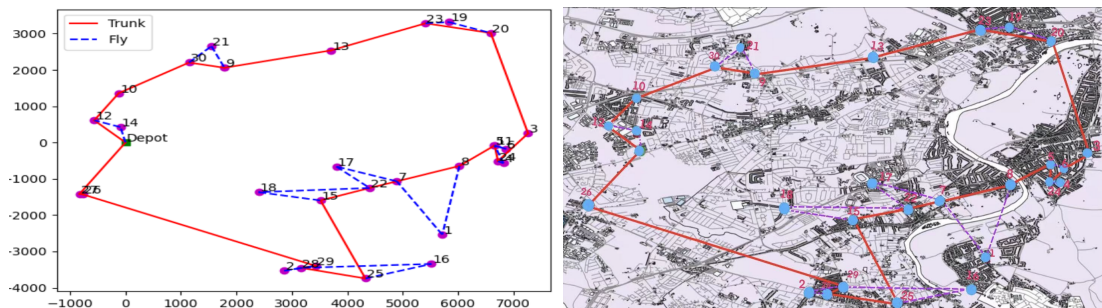


Figure 1 – Risk-aware vehicle routes

We present the routing optimization results in Figure 1, indicating that the riskiest customer nodes were not dispatched by drones. The predicted total operation time was 97 minutes, with 10 customer nodes visited by drones.

Table 1 – Comparison Between Different Vehicle Routing Models

Vehicle routing models	Truck-only	Truck-drone	Risk-aware truck-drone
Truck travel distance (kilometers)	45.34	27.29	29.07
Drone travel distance	0	30.89	25.15
Number of drone routes	0	11	10
Total travel time (minutes)	151.13	90.97	96.88

A comparison was made between a risk-unaware truck-only model, a risk-unaware truck-drone model, and a risk-aware truck-drone model in Table 1. One can see that disregarding risk resulted in a 20% longer distance traveled by the drone and a slightly faster delivery. Interestingly, both drone-based delivery models provided 35% time savings compared to the truck-only model.

Using the optimal customer visiting routes, we applied the Dijkstra algorithm to optimize drone paths. The comparison between optimized drone paths and those without the risk model

